Investigation of Oscillating Riblets for Turbulent Drag Reduction

F. Kramer, F. Thiele and E. Wassen
Technische Universität Berlin, Institut für Strömungsmechanik und Technische Akustik, Müller-Breslau-Str. 8, 10623 Berlin, Germany

Abstract

Results from direct numerical simulations show that stationary, blade-shaped riblets reduce turbulent friction drag by 8.6%. Tilting the riblets sinusoidally at an oscillation period of $T^+ = 35$, improves the drag reduction up to 11.1% compared to a smooth reference wall. The main improvement is found at the positions of maximal riblet tilting. Mean flow and fluctuation profiles are consistent with the observed difference in drag reduction between both configurations. Even though the oscillation increases the wall-normal motion this has no adverse effect on the drag. A visualization of vortex structures reveals much less vortical activity at the riblet surfaces.

1. Introduction

Riblets are a *passive* technique which has already been successfully applied in commercial products. Many different shapes have been investigated by, for example, Walsh[15] and Bechert[2]. The best results were obtained for blade-shaped riblets leading up to a drag reduction of 10%. On the other hand, a laterally oscillating smooth wall which was investigated by many authors[8;11;1;14;5] achieves a drag reduction up to 45%[4]. However, this *actively* driven method is very energy-consuming because a strong displacement of the wall is needed to induce an effective lateral motion. This motion reduces the streak and burst activity in the boundary layer[13;9] and hampers the streamwise vortices.

Combining the very effective oscillating wall with stationary riblets allows to induce lateral momentum at a certain distance from the wall[16] at much less expense.

2. Setup

Direct numerical simulations are performed in a fully turbulent channel at $Re_\tau = 360$, based on the shear velocity u_τ and the channel height H. The dimensions of the channel are depicted in figure 1. In streamwise direction, the channel's length is $3H$, and its width in spanwise direction is $1.5H$. A constant streamwise pressure gradient drives the newtonian and incompressible fluid through the channel which consists of two opposing surfaces. The top surface is a smooth wall for reference purposes whereas the bottom wall carries the blade-shaped riblet surface which consists of 32 riblet segments. Both surfaces are impermeable and have no slip. The sides of the channel normal to the streamwise and spanwise direction are periodic boundaries. Depending on time and investigated surface, the resulting Reynolds number based on the bulk velocity u_b varies between 5700 and 5900. Although the channel is not completely de-correlated[10], it is significantly larger than the "minimal flow unit"[7] and allows to simulate near wall structures of turbulent flow.

At least 410 convective units based on the time-averaged bulk-velocity and the channel height are used for the time-averaged data in this paper. The flow is computed on a structured grid of 11 million cells using a finite-volume discretization of second order accuracy in time and space.

The geometrical setup of the riblets agrees well with the optimal stationary riblets according to Bechert[3]. The height of the riblets, $h^+ = h\frac{u_\tau}{\nu}$, is 8.96 wall units, and the spacing between two adjacent riblets, $s^+ = s\frac{u_\tau}{\nu}$, is 16.875 wall units where ν denotes the kinematic viscosity. For the oscillating case, the riblets on the bottom surface are tilted sinusoidally up to a maximum angle of 30° while keeping the riblets stiff and synchronized.

The results from two simulations are presented in this paper. The first case uses stationary riblets. The second case has the same dimensions but the riblets are oscillating with a period of oscillation of $T^+ = T_{osc}u_\tau^2/\nu = 35$.

3. Drag reduction

The friction drag difference is calculated by integrating the wall shear stress of the top and the bottom wall separately. The relative drag reduction which is the averaged drag difference normalized by the top wall's drag

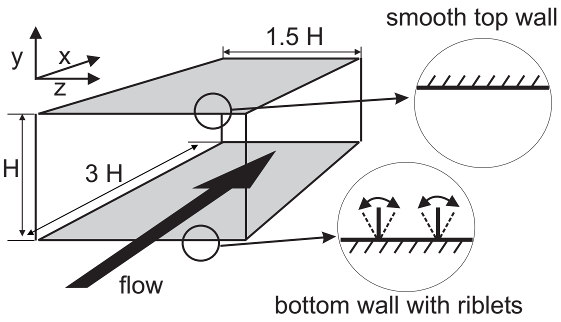

Figure 1: Computational domain.

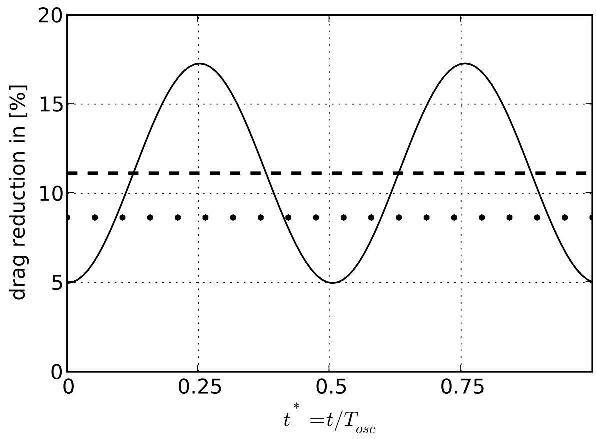

Figure 2: Drag reduction of both cases over phase angle where applicable; —— oscillating case, – – – time-average of oscillating case, · · · · · time-average of stationary case.

is plotted for both cases in figure 2. The abscissa t^* is the relative phase angle which depicts the development of the drag reduction over one period of oscillation, and is only meaningful for the oscillating case. The two horizontal lines indicate the time-averaged drag reduction of the stationary case achieving 8.6% and of the oscillating case improving the drag reduction to 11.1%. Comparing the oscillating case to the stationary case, it shows smaller drag reduction for the phase angles $t^* = 0$ and 0.5 and strong reduction improvements for 0.25 and 0.75. The former angles correspond to riblets in upright position whereas the latter angles correspond to riblets at the maximum tilting angle. Relative to the stationary case, this means that when being in upright position the drag is increased, and when being maximal tilted the drag is reduced.

4. Time-averaged flow

The time- and ensemble-averaged streamwise velocity profiles for both cases are shown in figures 3 and 4. For comparison, the law of the wall is also given in these figures. Figure 3 shows the velocity profiles at the midpoint between the riblets. The dashed line representing the oscillating riblets in vertical position is slightly elevated in the lower buffer layer compared to the stationary riblets. Because the drag is directly linked to the slope of the velocity profile at the wall, this is consistent with a smaller drag reduction at that phase angle. The drag reduction is improved for the maximal tilting angle which is demonstrated in this figure by the dash-dotted line being slightly below the stationary riblets. Compared to the laws of the wall, all three profiles show a significantly lower velocity in the lower buffer layer and an increased velocity in the logarithmic region. This increase is the direct result of the reduced skin friction because the constant driving pressure gradient accelerates the flow.

The velocity profiles in figure 4 are plotted in wall-normal direction starting at the riblet root. Because of the presence of the riblets the profiles of the stationary and the oscillating riblets at $t^* = 0$ end at the riblet tips. Both profiles show no major difference and are nearly identical. In terms of drag reduction, the velocity profile of the oscillating case at $t^* = 0.25$ is much more improved above the riblet root than above the midpoint in figure 3.

5. Wall-normal motion

Fluid motion perpendicular to the wall is generally considered to increase the drag because it also increases the transport of momentum to and away from the wall. Even stationary riblets produce, only because of their geometrical shape, a weak wall-normal motion as given in figure 5. The contours over a riblet cross section show the wall-normal velocity component normalized by the shear velocity u_τ. A downward motion can be observed above the riblet valley which is about 1% of the streamwise velocity at this height. It is accompanied by a comparable upward motion above the riblet tips.

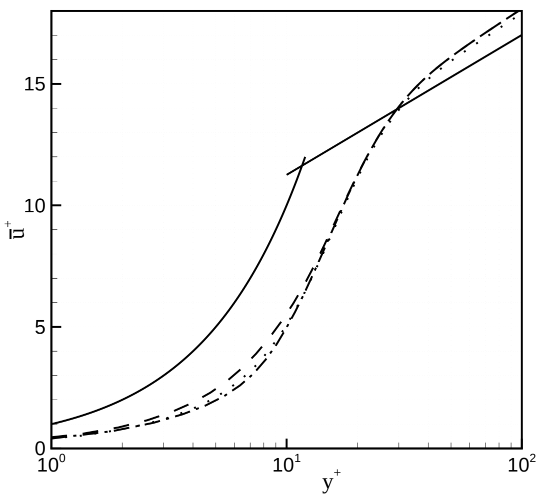

Figure 3: Mean velocity profiles at the midpoint between riblets; $\cdots\cdots$ stationary riblets, $---$ $T^+ = 35$ at $t^* = 0$, $-\cdot-\cdot-$ $T^+ = 35$ at $t^* = 0.25$, —— laws of the wall ($u^+ = y^+$ and $u^+ = 2.5 \ln y^+ + 5.5$).

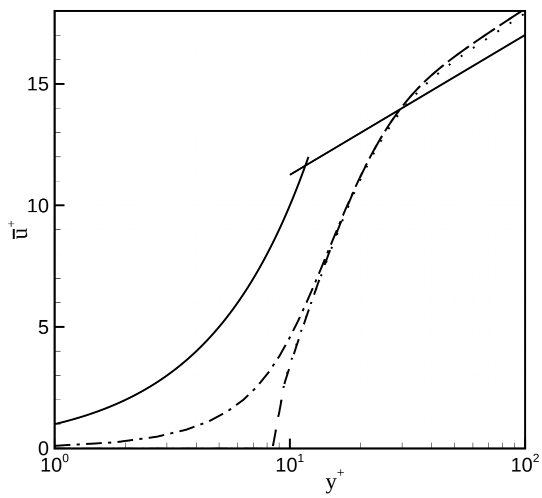

Figure 4: Mean velocity profiles at the riblet location; $\cdots\cdots$ stationary riblets, $---$ $T^+ = 35$ at $t^* = 0$, $-\cdot-\cdot-$ $T^+ = 35$ at $t^* = 0.25$, —— laws of the wall ($u^+ = y^+$ and $u^+ = 2.5 \ln y^+ + 5.5$).

Figure 6 plots contours from phase-averaged data of the oscillating case at a phase-angle of 0°. Since it uses the same contour levels as figure 5, the strong difference between both cases is evident. The downward motion above the riblet valley has increased to about 4% of the streamwise velocity at this height. Even at the maximum tilting angle in figure 7 it is still about 3%. These results indicate that wall-normal motion is not necessarily drag increasing but can even have the inverse effect.

6. Turbulence and streamwise vortices

Turbulent activity is largely dominated by the fluctuation of the streamwise velocity component. A drag reducing configuration should dampen the fluctuations, as can be seen in figure 8. Below $y^+ = 25$, all riblet fluctuation profiles are much weaker than the smooth reference wall from the stationary riblet case. As already observed for the velocity profiles, the fluctuations of the oscillating case are slightly stronger than those of the stationary riblets for $t^* = 0$, and they are slightly weaker for $t^* = 0.25$. This consistent behaviour is also present in figure 9 which shows the fluctuation profiles above the riblet root. The oscillating case at $t^* = 0$ and the stationary riblets collapse onto the same profile. But at $t^* = 0.25$, a strong improvement compared to all midpoint profiles in figure 8 can be observed.

Vortex cores can be visualized by iso-surfaces of the vortex indicator q. A 3D snapshot of the stationary riblet case with iso-surfaces of $q = 5$ in figure 10 shows large clusters of complex vortical structures at the smooth top wall. Indicating the direction of rotation, dark-gray surfaces mean positive streamwise vorticity whereas light-gray surfaces stand for negative streamwise vorticity. Stationary riblets are considered to hamper cross motion and streamwise vortices. Consequently, the bottom wall which is covered by riblets produces less vortices, and the clustering is less pronounced. The riblets' influence can be clearly distinguished.

An arbitrarily chosen snapshot of the oscillating case at $t^* = 0$ is shown in figure 11. As for the stationary riblets, the smooth top wall produces larger and stronger clusters than the riblet surface. At the bottom wall, vortices which correspond to the strongly increased wall-normal motion can be observed at the riblet tips.

7. Conclusion

Oscillatory tilting of riblets has the capability to improve drag reduction beyond the stationary optimum. The gain is mainly found at the maximum tilting positions which is supported by the analysis of velocity and velocity fluctuation profiles. The investigation of secondary motion indicate a positive effect of stronger wall-normal motions.

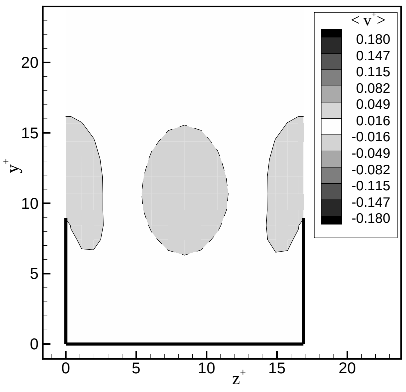

Figure 5: Contours of time-averaged wall-normal velocity for the stationary riblets. Dashed lines indicate negative values.

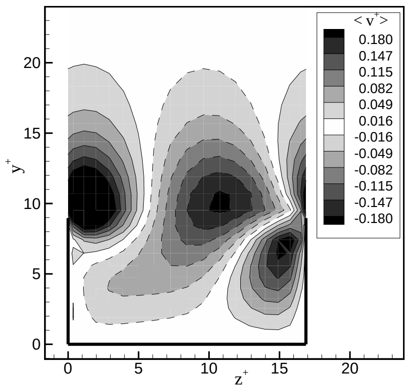

Figure 6: Contours of phase-averaged wall-normal velocity for the oscillating case at $t^* = 0$. Dashed lines indicate negative values.

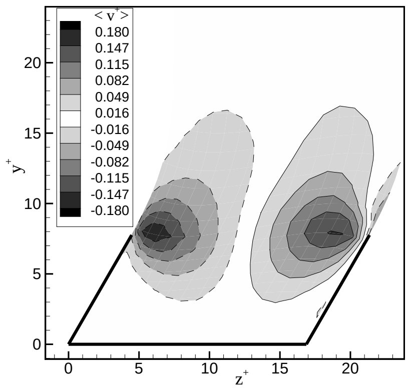

Figure 7: Contours of phase-averaged wall-normal velocity for the oscillating case at $t^* = 0.25$. Dashed lines indicate negative values.

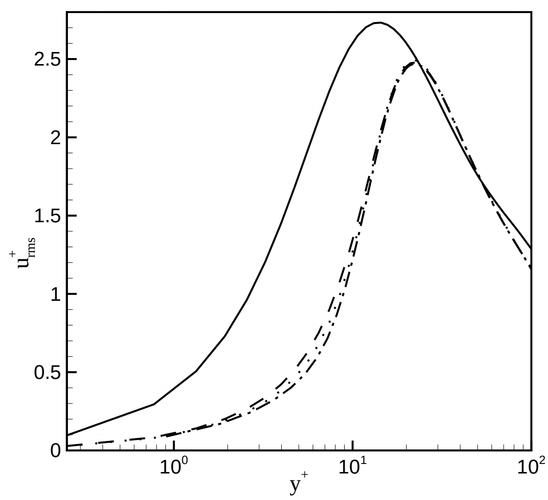

Figure 8: Streamwise velocity fluctuation profiles at the midpoint between riblets; $\cdots\cdots$ stationary riblets, $---$ $T^+ = 35$ at $t^* = 0$, $-\cdot-\cdot-$ $T^+ = 35$ at $t^* = 0.25$, —— smooth wall.

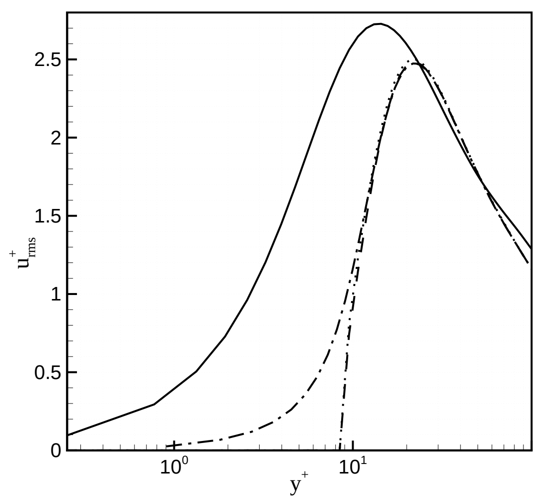

Figure 9: Streamwise velocity fluctuation profiles at the riblet location; $\cdot\cdot\cdot\cdot\cdot$ stationary riblets, $---$ $T^+ = 35$ at $t^* = 0$, $-\cdot-\cdot-$ $T^+ = 35$ at $t^* = 0.25$, —— smooth wall.

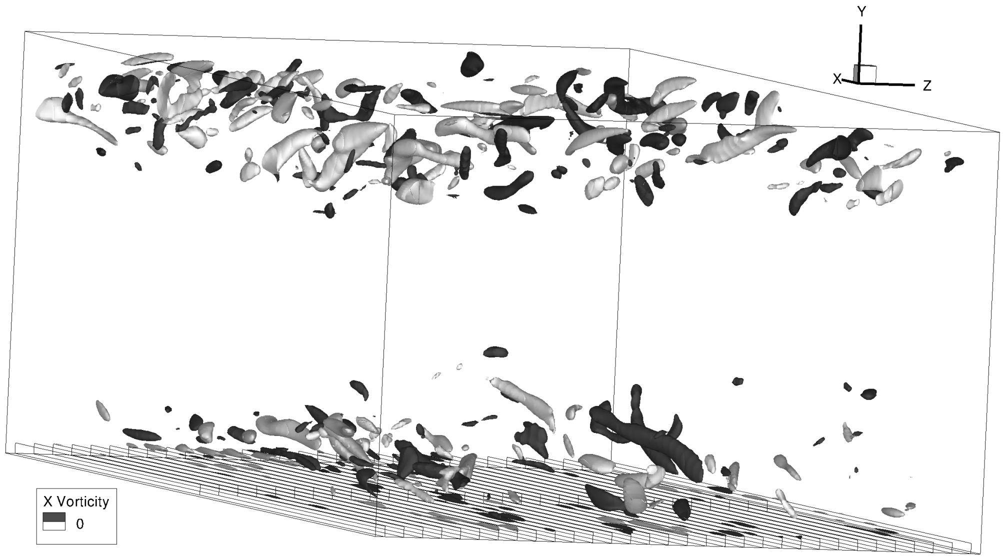

Figure 10: Iso-surfaces of $q = 5$ for a 3D snapshot of the stationary riblets; dark-gray: positive streamwise vorticity, light-gray: negative streamwise vorticity.

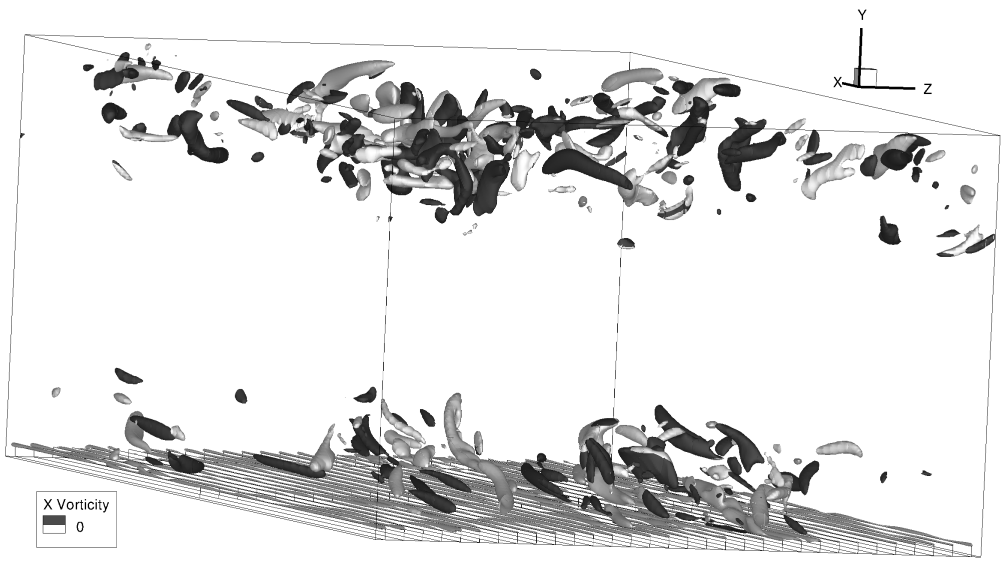

Figure 11: Iso-surfaces of $q = 5$ for a 3D snapshot of the oscillating riblets; dark-gray: positive streamwise vorticity, light-gray: negative streamwise vorticity.

8. Acknowledgments

This research was funded by the German Science Foundation (DFG) within the scope of the priority program Nature-Inspired Fluid Mechanics (SPP 1207). The simulations were performed on the National Supercomputer HLRB II (SGI Altix 4700) at the Leibniz-Rechenzentrum (LRZ), Munich, Germany.

References

[1] Baron, A. and Quadrio, M., "Turbulent drag reduction by spanwise wall oscillations," *Applied Scientific Research*, vol. 55, pp. 311-326, 1996.

[2] Bechert, D.W. and Bartenwerfer, M., "The viscous flow on surfaces with longitudinal ribs," *J. Fluid Mech.*, vol. 206, pp. 105-129, 1989.

[3] Bechert, D.W., Bruse, M., Hage, W., van der Hoeven, J.G.T., and Hoppe, G., "Experiments on drag-reducing surfaces and their optimization with an adjustable geometry," *J. Fluid Mech.*, vol. 338, pp. 59-87, 1997.

[4] Choi, K.S., DeBisschop, J.-R., and Clayton, B.R., "Turbulent boundary-layer control by means of spanwise-wall oscillations," *AIAA Journal*, vol. 36 (7), pp. 1157-1163, 1998.

[5] Choi, K.S. and Clayton, B.R., "The mechanism of turbulent drag reduction with wall oscillation," *Int. J. Heat and Fluid Flow*, vol. 22, pp. 1-9, 2001.

[6] Frohnapfel, B. and Lammers, P. and Jovanovic, J. and Durst, F., "Interpretation of the mechanism associated with turbulent drag reduction in terms of anisotropy invariants", *J. Fluid Mech.*, vol. 577, pp. 457-466, 2007.

[7] Jiménez, J. and Moin, P., "The minimal flow unit in near-wall turbulence," *J. Fluid Mech.*, vol. 225, pp. 213-240, 1991.

[8] Jung, W.J., Mangiavacchi, N., and Akhavan, R., "Suppression of turbulence in wall-bounded flows by high-frequency spanwise oscillations," *Phys. Fluids A*, vol. 4 (8), pp. 1605-1607, 1992.

[9] Karniadakis, G.E. and Choi, K.S., "Mechanisms on transverse motions in turbulent wall flows," *Annu. Rev. Fluid Mech.*, vol. 35, pp. 45-62, 2003.

[10] Kim, J., Moin, P., and Moser, R., "Turbulence statistics in fully developed channel flow at low Reynolds number," *J. Fluid Mech.*, vol. 177, pp. 133-166, 1987.

[11] Laadhari, F., Skandaji, L., and Morel, R., "Turbulence reduction in a boundary layer by a local spanwise oscillating surface," *Phys. Fluids*, vol. 6 (10), pp. 3218-3220, 1994.

[12] Luchini, P., Manzo, F., and Pozzi, A., "Resistance of a grooved surface to parallel flow and cross-flow," *J. Fluid Mech.*, vol. 228, pp. 87-109, 1991.

[13] Miyake, Y., Tsujimoto, K., and Takahashi, M., "On the mechanism of drag reduction of near-wall turbulence by wall oscillation," *JSME Int. Journal, Series B*, vol. 40 (4), pp. 558-566, 1997.

[14] Trujillo, S.M., Bogard, D.G., and Ball, K.S., "Turbulent boundary layer drag reduction using an oscillating wall," *AIAA Paper 97-1870*, 1997.

[15] Walsh, M.J., "Riblets," *Prog. Astronaut. Aeronaut.*, vol. 123, pp. 203-261, 1990.

[16] Wassen, E., et al., "Turbulent drag reduction by oscillating riblets," *AIAA 4th flow control conference*, AIAA-2008-3771, 2008.